Developmental Cell, Vol. 1, 515–525, October, 2001, Copyright ©2001 by Cell Press

The Role of Dynamin-Related Protein 1, a Mediator of Mitochondrial Fission, in Apoptosis

**Stephan Frank,[1] Brigitte Gaume,[1]
Elke S. Bergmann-Leitner,[2] Wolfgang W. Leitner,[3]
Everett G. Robert,[1] Frédéric Catez,[4]
Carolyn L. Smith,[5] and Richard J. Youle[1,6]**

[1] Biochemistry Section
Surgical Neurology Branch
National Institute of Neurological Disorders and Stroke
[2] Laboratory of Tumor Immunology and Biology
National Cancer Institute
[3] Surgery Branch
National Cancer Institute
[4] Protein Section Center for Cancer Research
National Cancer Institute
[5] Light Imaging Facility
National Institute of Neurological Disorders and Stroke
National Institutes of Health
Bethesda, Maryland 20892

Summary

In healthy cells, fusion and fission events participate in regulating mitochondrial morphology. Disintegration of the mitochondrial reticulum into multiple punctiform organelles during apoptosis led us to examine the role of Drp1, a dynamin-related protein that mediates outer mitochondrial membrane fission. Upon induction of apoptosis, Drp1 translocates from the cytosol to mitochondria, where it preferentially localizes to potential sites of organelle division. Inhibition of Drp1 by overexpression of a dominant-negative mutant counteracts the conversion to a punctiform mitochondrial phenotype, prevents the loss of the mitochondrial membrane potential and the release of cytochrome c, and reveals a reproducible swelling of the organelles. Remarkably, inhibition of Drp1 blocks cell death, implicating mitochondrial fission as an important step in apoptosis.

Introduction

In multicellular organisms, programmed cell death (apoptosis) ensures the precise and orderly elimination of surplus or seriously damaged and potentially harmful cells. Cells destined to die by apoptosis display typical morphological alterations with plasma membrane blebbing and nuclear condensation/fragmentation usually occurring during the penultimate stages of cell life (White, 1996). Although various cell death signaling pathways are critically dependent on mitochondria (Susin et al., 1998), not much is known about the dynamic morphological changes that reflect the involvement of these organelles. Mitochondria may (Matsuyama et al., 2000; Petit et al., 1998; Scarlett et al., 2000; Vander Heiden et al., 1997) or may not (Jürgensmeier et al., 1998; Kluck et al., 1999; Martinou et al., 1999) respond to apoptotic stimuli by swelling. According to one mechanistic model, swelling of the mitochondrial matrix is causally associated with the loss of the mitochondrial membrane potential ($\Delta\psi_m$) and perturbed outer mitochondrial membrane integrity, followed by the subsequent release of apoptogenic intermembrane space proteins (such as certain procaspases, AIF, cytochrome c, Smac/DIABLO) into the cytosol. This cascade of events appears to culminate in the activation of cytosolic effector proteases (caspases) (Green and Reed, 1998; Kroemer and Reed, 2000). In addition, antiapoptotic members of the Bcl-2 family such as Bcl-2 and Bcl-X_L are known to exert their function, at least partly, by negatively regulating this process (Gross et al., 1999; Kluck et al., 1997; Vander Heiden et al., 1997; Vander Heiden and Thompson, 1999; Yang et al., 1997).

We report here that after a transient phase of organelle stretching, the typical reticular arrangement of mitochondria of healthy living COS-7 cells disintegrates dramatically into small punctiform mitochondria during cell death induced by various apoptotic stimuli. The same phenomenon, speculated to be consistent with mitochondrial fragmentation, has recently been observed upon overexpression of Bax (Desagher and Martinou, 2000). As mitochondrial length is the net product of fusion and fission events, we hypothesized that the small punctiform mitochondrial phenotype during apoptosis might result from an activation of physiological fission. Interestingly, recent studies have shown that certain dynamins are involved in these processes.

First described more than a decade ago (Shpetner and Vallee, 1989), dynamins have been conventionally associated with receptor-mediated endocytosis at the plasma membrane. Since then, a picture has emerged in which dynamins belong to a superfamily of large GTPase proteins that function at various intracellular localizations (recently reviewed by Hinshaw, 2000; McNiven et al., 2000; van der Bliek, 1999). Besides their role in mediating endocytosis, dynamins are now increasingly being recognized for their role in vesicle formation from compartments such as the endoplasmic reticulum and the Golgi apparatus, implicating them in the essential physiological processes of ER-Golgi- and Golgi-vacuole membrane trafficking. However, the question of how dynamin proteins exert their functions has not yet been answered completely. It has been demonstrated that dynamin assembles into multimeric spirals around the neck of nascent endocytic vesicles (Takei et al., 1995), which subsequently may be pinched off either by constriction (Sweitzer and Hinshaw, 1998) or by changes of the helical pitch (Stowell et al., 1999). Alternatively, results of another study suggest an indirect involvement of dynamin, functioning as a signaling molecule by recruiting other, force-generating molecule(s) to the site of action (Sever et al., 1999).

Several lines of evidence suggest that certain dynamin family members may also be involved in the regulation of membrane scission of mitochondria. First, a novel dynamin-related protein, Drp1 (described by several

[6] Correspondence: youler@ninds.nih.gov

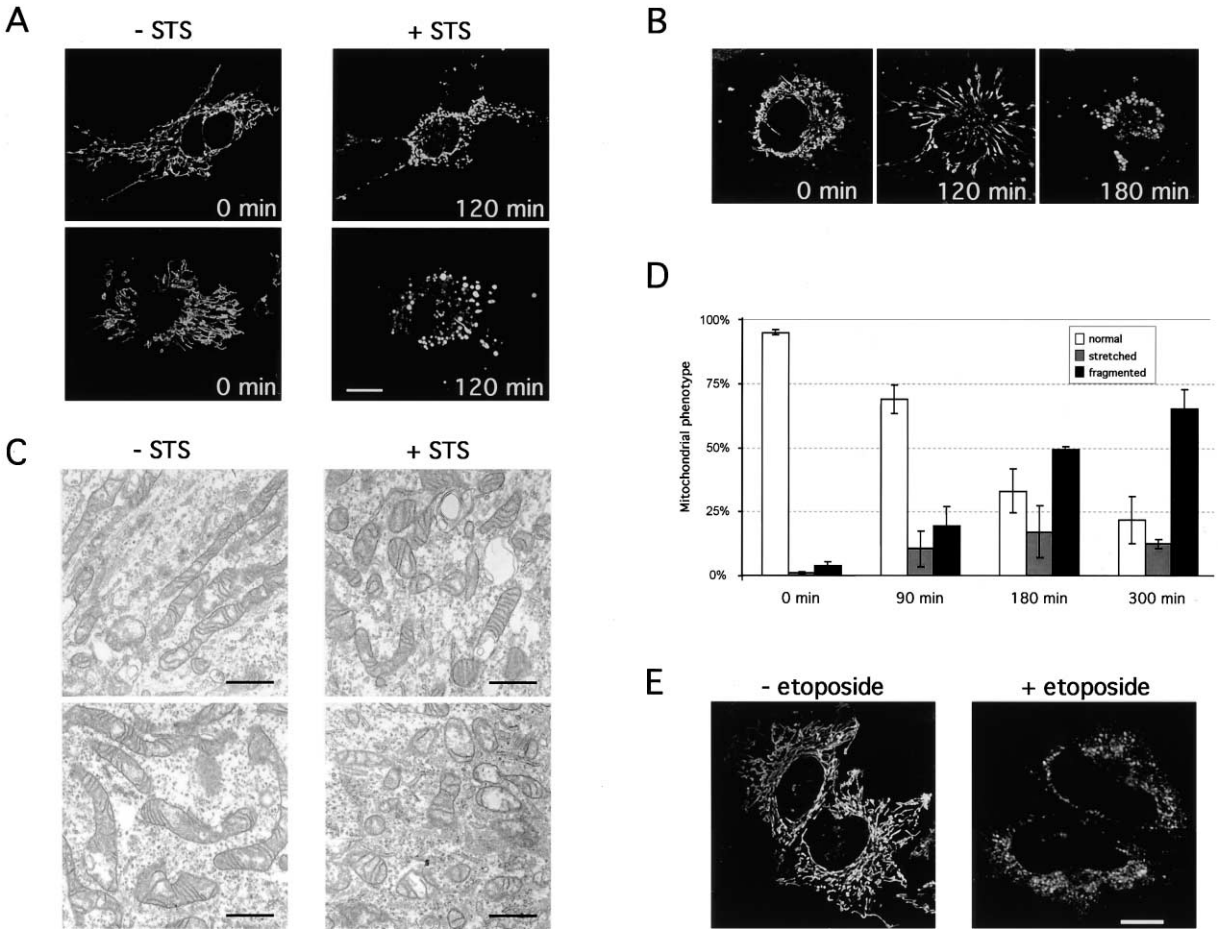

Figure 1. The Conversion of the Reticulo-Tubular Mitochondrial Morphology into a Punctiform Phenotype during Apoptosis

COS-7 cells transfected with mito-GFP were treated with the nonselective kinase inhibitor staurosporine (1.2 μM) to induce apoptosis and visualized by confocal microscopy. To prevent cell detachment and to better maintain cellular morphology, cells were pretreated with the caspase inhibitor Z-VAD-fmk. Quantitative experiments have shown that there is no difference in the mitochondrial fragmentation rate of Z-VAD-fmk-pretreated cells versus controls.

(A) Two cells undergoing profound changes of their mitochondrial phenotype during STS-induced apoptosis are shown. In both cells, the characteristic reticulo-tubular mitochondrial morphology disintegrates into numerous round fragments of varying size. In some cells, as exemplified by the bottom panel, the resulting punctiform mitochondria appear swollen, relative to the normally thin diameter of the mitochondrial tubules.

(B) Stretching precedes the morphological disintegration of the mitochondrial reticulum after STS treatment. Scale bar, 20 μm.

(C) Dimensions of mitochondrial organelles were quantified by electron microscopy using NIH Image software (version 1.62). Mitochondria of healthy cells (left) are significantly longer in length (1.87 ± 1.35 μm; $n = 129$) as compared to mitochondria of cells treated with 1.2 μM STS for 3 hr (0.86 ± 0.37 μm; $n = 116$; Wilcoxon Test, $p < 0.00001$). Scale bar, 1 μm.

(D) Mitochondrial morphology of COS-7 cells ($n > 150$) was assessed at the indicated time points after STS addition by confocal microscopy. The gradual decrease in the percentage of cells featuring normal mitochondrial morphology is paralleled by an increasing percentage of cells exhibiting the punctiform phenotype. Mitochondrial stretching is a transient phenomenon.

(E) Mitochondrial morphology was also documented in mito-GFP transfected HeLa cells before (left) and after 32 hr of etoposide treatment (right; 500 μM). Scale bar, 20 μm.

groups as Drp1 [Imoto et al., 1998], DLP1 [Yoon et al., 1998], DVLP [Shin et al., 1997], and Dymple [Kamimoto et al., 1998]), has been shown to regulate mitochondrial morphology in mammalian cells without affecting transport functions of the secretory and endocytic pathways (Pitts et al., 1999; Smirnova et al., 1998). In particular, overexpression of a dominant-negative mutant (harboring an inactive GTPase domain) in mammalian cells produced a peculiar mitochondrial phenotype marked by an increased tendency of the organelles to form highly interconnected mitochondrial aggregates (Smirnova et al., 1998, 2001; van der Bliek, 2000). Furthermore, studies in *C. elegans* have revealed that Drp1 specifically controls severing of the mitochondrial outer membrane during organelle fission with dominant negative Drp1 mutants inhibiting membrane scission (Labrousse et al., 1999). Finally, mitochondrial division in yeast depends on Dnm1, a protein homologous to Drp1 (Bleazard et al., 1999; Mozdy et al., 2000; Otsuga et al., 1998; Sesaki and Jensen, 1999).

Here we provide evidence that, during apoptosis, Drp1 not only regulates the transition from a reticulotubular to a punctiform mitochondrial phenotype but is also involved in mitochondria-dependent cell death, suggesting a novel role for proteins of the dynamin family.

Results

The Conversion from the Reticulo-Tubular to a Punctiform Mitochondrial Phenotype during Apoptosis

By confocal microscopy we observed that mitochondria of early apoptotic cells undergo various structural changes. To visualize these changes, COS-7 cells were transiently transfected with a green fluorescent protein/cytochrome c oxidase subunit VIII fusion construct (mito-GFP) that specifically targets the mitochondrial matrix compartment (Rizzuto et al., 1992). At 20 hr after transfection, cells were either incubated with various inducers of established cell death pathways (e.g., staurosporine, etoposide) or exposed to γ irradiation to elicit a mitochondria-dependent apoptotic response. We found that after induction of apoptosis, the typical tubular mitochondrial phenotype of healthy cells (see Supplemental Figures S1 and S2 [http://www.developmentalcell.com/cgi/content/full/1/4/515/DC1]) disintegrates into small, rounded and sometimes spherical organelles (Figure 1). The number of individual mitochondria increased 2.1 $\pm$ 0.29-fold in these cells, suggesting a model whereby mitochondrial fission participates in the transition between these two distinct mitochondrial phenotypes during apoptosis. However, we cannot exclude mitochondrial condensation as a possible concomitant component of this process. Using electron microscopy, we measured mitochondrial dimensions and found a marked decrease in the average length of the organelles 3 hr after induction of apoptosis, consistent with this model (Figure 1C). In addition, the conversion between the two distinct mitochondrial phenotypes during apoptosis was demonstrated by three-dimensional reconstruction of serial (z axis) images (see Supplemental Data [http://www.developmentalcell.com/cgi/content/full/1/4/515/DC1] for movie explanation).

As exemplified by Figure 1B, we also found that mitochondria often stretch prior to the occurrence of punctiform organelles. This sequence of events was quantitatively analyzed with time after apoptosis induction (Figure 1D) and is additionally documented by a movie showing mitochondrial stretching and subsequent division into multiple separate mitochondria in two adjacent (mito-GFP transfected) COS-7 cells during staurosporine (STS) treatment (see Supplemental Data). The conversion from a tubular to a punctiform mitochondrial phenotype occurs in essentially all apoptotic COS-7 cells. Mitochondrial stretching precedes this morphological change in at least 60% of the cells. We also documented the occurrence of punctiform mitochondria in various other cell lines following treatment with different apoptotic stimuli (HeLa cervical carcinoma cells [STS, cisplatin, etoposide; Figure 1E], 9L and C6 glioma cells [STS], RD rhabdomyosarcoma cells [STS]; data not shown), and, therefore, the punctiform mitochondrial phenotype appears to represent a general morphological correlate to apoptosis.

Bax Accelerates the Transition between the Two Mitochondrial Phenotypes

Various Bcl-2 proteins have been implicated in the mitochondrial regulation of apoptosis (Adams and Cory, 1998; Gross et al., 1999; Kroemer, 1997). To examine the role of proapoptotic Bcl-2 family members in the mitochondrial phenotype conversion, we tested whether overexpression of Bax, a protein that redistributes from the cytosolic compartment to the mitochondria during apoptosis (Gross et al., 1998; Hsu et al., 1997; Wolter et al., 1997), would have any effect on organelle fragmentation. Blinded quantitative assessment of mitochondrial morphology by monitoring single cells before and 75 min after STS treatment revealed that the occurrence of punctiform organelles was greatly accelerated in cells overexpressing full-length Bax (Figure 2). Even without STS treatment, Bax overexpression promoted the punctiform phenotype (Figure 2) and apoptosis (data not shown). The Bcl-2 homology domain 3 (BH3) of proapoptotic Bcl-2 family members has been causally linked to the proapoptotic properties of these proteins (Adams and Cory, 1998; Gross et al., 1999; Wang et al., 1998). Therefore, we also tested a Bax mutant lacking the BH3 domain. No acceleration of fragmentation with this deletion mutant was observed (Figure 2). Thus, transient overexpression of full-length Bax significantly accelerates the disintegration of the mitochondrial reticulum, further linking the profound changes in the phenotype of the organelles with apoptotic cell death.

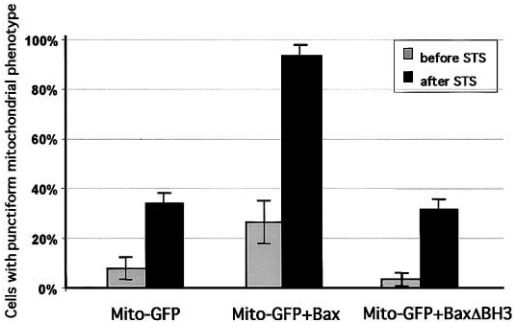

Figure 2. Bax Expression Accelerates the Changes in Mitochondrial Morphology

Mitochondrial morphology was assessed by blinded quantification of confocal microscopy pictures before and after STS treatment in COS-7 cells either transfected with mito-GFP (left), cotransfected with mito-GFP and pcDNA3-Bax (middle), or mito-GFP plus BaxΔBH3 (right). In each of three independent experiments, the mitochondrial morphology of more than 100 randomly selected cells was assessed and their x-y coordinates recorded. After 75 min of STS exposure, mitochondrial morphology of the same cells was reassessed. Cells overexpressing full-length Bax show the punctiform phenotype significantly more often in comparison to control cells or cells overexpressing BaxΔBH3.

Dynamin-Related Protein 1 Redistributes to Mitochondrial Membranes during Apoptosis

Recent studies have revealed that a novel member of the dynamin family, Drp1, is involved in outer mitochondrial membrane scission (Labrousse et al., 1999). As wild-type Drp1 cycles on and off sites of mitochondrial division in healthy cells, we examined its subcellular localization during apoptosis. In healthy mammalian cells, Drp1 has primarily a cytosolic subcellular distribution (Kamimoto et al., 1998; Shin et al., 1997; Smirnova et al., 1998; Smirnova et al., 2001). Monitoring GFP-Drp_{wt} transfected COS-7 cells during the early stages of apoptosis, we found that, prior to the onset of mitochondrial fragmentation, GFP-Drp_{wt} redistributes from diffuse

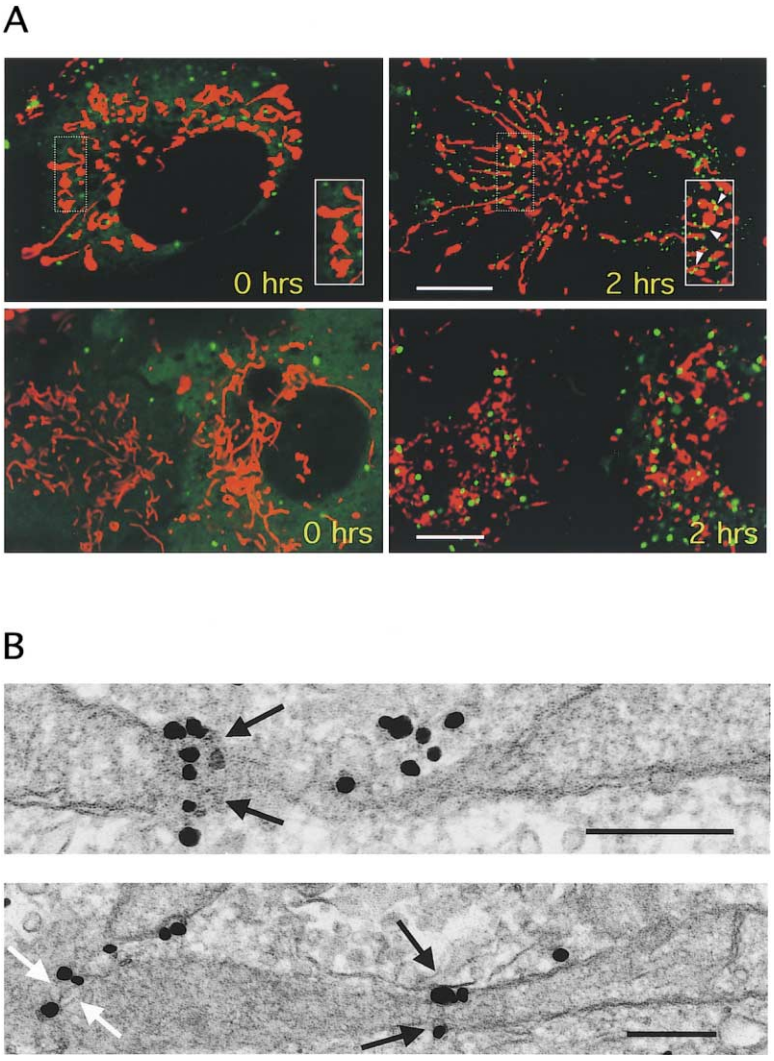

Figure 3. Drp1 Translocates to the Mitochondria during Apoptosis

(A) In healthy COS-7 cells (upper left panels), most of the GFP-Drp_{wt} has a diffuse cytosolic distribution (mitochondria stained with MitoTracker). During apoptosis (1.2 μM STS for 2 hr), cytosolic GFP-Drp_{wt} partially redistributes to small foci along the surface of mitochondria, at mitochondrial constriction sites and at the tips of individual mitochondria (upper right panels; arrowheads in inset). In addition, some cytosolic Drp1 appears partially punctate which might reflect colocalization with either endoplasmic reticulum (Yoon et al., 1998) or with punctiform mitochondria. Scale bar, 20 μm.

(B) Immunoelectron microscopy studies, performed under identical experimental settings, confirmed the preferential localization of GFP-Drp_{wt} at mitochondrial constriction sites (black arrows) and at the interface of adjacent mitochondria (white arrows); anti-GFP antibody from Qbiogene, Carlsbad, CA. Scale bar, 200 nm.

in the cytosol to become progressively punctate along the surface of mitochondria. The resulting distribution, visualized by confocal microscopy (Figure 3A) and by immunoelectron microscopy (Figure 3B), appears preferentially at sites of mitochondrial constriction and mitochondrial tips and thus is reminiscent of the Drp1 localization pattern during mitochondrial division in *C. elegans* (Labrousse et al., 1999). Whether or not apoptosis-associated mitochondrial stretching is a prerequisite for Drp1 localization at apoptotic mitochondria remains to be clarified.

Mitochondrial Fission and Swelling during Apoptosis Are Regulated by Drp1

Postulating that the translocation of Drp1 to mitochondria might reflect a function in outer mitochondrial membrane scission, we explored the effect of a dominant-negative mutant of Drp1, which blocks mitochondrial division in *C. elegans* (Labrousse et al., 1999), on mitochondrial morphology during apoptosis. Comparative monitoring of STS-treated cells using the mitochondrial matrix marker mito-GFP for organelle visualization revealed that cells cotransfected with the Drp_{K38A} mutant change their mitochondrial phenotype to a significantly lesser degree than cells expressing endogenous Drp1 (Figure 4). After 150 min of STS treatment, we found only a 1.02 ± 0.02-fold increase in the number of mitochondrial organelles in Drp_{K38A} overexpressing cells ($n = 5$), whereas a 2.1 ± 0.29-fold increase was observed in cells expressing Drp1 at the endogenous level ($n = 5$; Fisher's exact two-tailed t test, $p < 0.001$; see Supplemental Data). Since Drp1 selectively mediates scission of the outer mitochondrial membrane, we additionally quantified the difference in fragmentation rate by experiments in which mitochondria were labeled with YFP-$Baxtail_{\Delta 184}$, a marker that constitutively localizes to the outer mitochondrial membrane without affecting apoptosis (see Supplemental Figures S3 and S4; Nechushtan et al., 1999, 2001). Confocal microscopy images of COS-7 cells, cotransfected with YFP-$Baxtail_{\Delta 184}$ and either Drp_{wt} ($n = 88$) or Drp_{K38A} ($n = 74$), were taken before and after STS treatment (only cells with characteristic tubular mitochondrial morphology prior to STS treatment were chosen for imaging). Blinded scoring of the punctiform mitochondrial phenotype when at least 90% of the worm-like mitochondria of a cell were disinte-

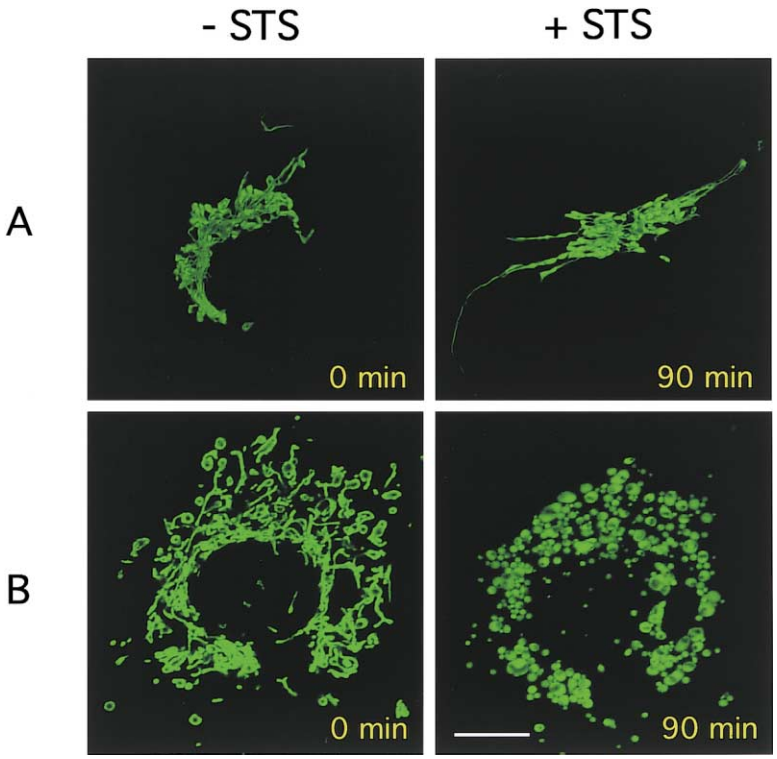

Figure 4. Expression of Dominant-Negative Drp1 (Drp_{K38A}) Prevents Mitochondrial Fission

COS-7 cells cotransfected with mito-GFP and Drp_{K38A} (A) or transfected with mito-GFP alone (B) were visualized by confocal microscopy at indicated time points during STS treatment (1.2 μM). Pictures shown here are projections of serial z axis images (0.2 μm increments; processed by LSM510 software); three-dimensional reconstructions are available online (http://www.developmentalcell.com/cgi/content/full/1/4/515/DC1).

(A) A mito-GFP/Drp_{K38A} cotransfected cell during apoptosis. Note the peculiar mitochondrial phenotype with highly interconnected single mitochondria and a few elongated organelles in these cells (Smirnova et al., 1998, 2001; van der Bliek, 2000). No mitochondrial disintegration but remarkable organelle stretching is observed.

(B) In control cells, the typical worm-like mitochondrial morphology disintegrates into numerous round, and sometimes spherical organelles of varying size under experimental conditions identical to (A). Scale bar, 20 μm.

grated substantiated a statistically highly significant difference in the mitochondrial fragmentation rates between Drp_{wt} transfected cells (73.9% of cells had punctiform mitochondria after 3 hr) versus Drp_{K38A} transfected cells (47.3% of cells with punctiform organelles after 3 hr; Fisher's exact two-tailed t test, $p < 0.001$). These findings show that expression of dominant-negative Drp1 inhibits the apoptosis-associated activation of outer mitochondrial membrane scission, thereby counteracting mitochondrial fission during cell death.

We also observed that the Drp_{K38A} mutant was capable of preventing mitochondrial fragmentation induced by overexpression of Bax (which accelerates conversion to the punctiform phenotype; Figure 2). Drp_{K38A} expression did not prevent translocation of Bax to mitochondria. Remarkably, mitochondria progressively enlarged but remained tubular (Figure 5A) and retained their membrane potential (Figure 5B). By measuring diameters of 15 randomly selected, worm-like mitochondria per cell before and 45 min after apoptosis induction (1.2 μM STS), we found that mitochondria in GFP-Bax/Drp_{K38A} cotransfected COS-7 cells ($n = 11$) became more than 1.6 times larger in diameter. In contrast, in the GFP-Bax/Drp_{wt} cotransfected controls ($n = 10$), a less than 1.2-fold increase in diameter was observed, the difference being highly statistically significant (nonpaired Wilcoxon test; $p = 0.0166$). By counteracting mitochondrial fission during apoptosis, overexpression of dominant-negative Drp1 enables organelle swelling to become apparent. Our findings show that two apoptosis-associated processes, mitochondrial fragmentation (blocked by inhibition of Drp1) and mitochondrial swelling (exacerbated by inhibition of Drp1), can be dissociated at the molecular level by their differential dependence on Drp1.

Dominant-Negative Drp1 Inhibits Apoptosis-Associated Inner Mitochondrial Membrane Depolarization and Cytochrome C Release

The intracellular redistribution of Drp1 during apoptosis together with the Drp_{K38A}-mediated block of mitochondrial fission led us to consider whether Drp1 might participate in apoptosis. Depolarization of the inner mitochondrial membrane potential (loss of $\Delta\psi_m$) in conjunction with perturbed outer membrane integrity is considered an important event occurring early during apoptosis (for review see Kroemer and Reed, 2000). To analyze the relationship between mitochondrial fragmentation and loss of $\Delta\psi_m$, we exposed mito-GFP transfected cells to the membrane potential-sensitive dye MitoTracker. Upon induction of apoptosis with STS, we found that mitochondria lose MitoTracker staining during fragmentation (Figure 6A). In contrast to most punctiform organelles, stretched mitochondria usually retain their membrane potential (Figure 6A). To test the role of Drp1 in the decrease in membrane potential, loss of $\Delta\psi_m$ was quantified by flow cytometry using the $DiOC_6(3)$ assay (Kluck et al., 1997; Kroemer et al., 1998; Scaffidi et al., 1998; Susin et al., 1997; Zamzami et al., 1995). We found that Drp_{wt} transfected COS-7 cells have a significantly reduced $\Delta\psi_m$ after about 5 hr of STS treatment (Figure 6B). In these cells, loss of $\Delta\psi_m$ appeared to be complete at about 8 hr of STS treatment. In contrast, in Drp_{K38A} transfected cells, the decrease in membrane potential occurred at a much lower rate (Figure 6B). Almost identical results were obtained when apoptosis was induced solely by overexpression of the pro-apoptotic Bcl-2 homolog Bax (data not shown), suggesting that Drp1 is required for the loss of $\Delta\psi_m$ in several cell death pathways.

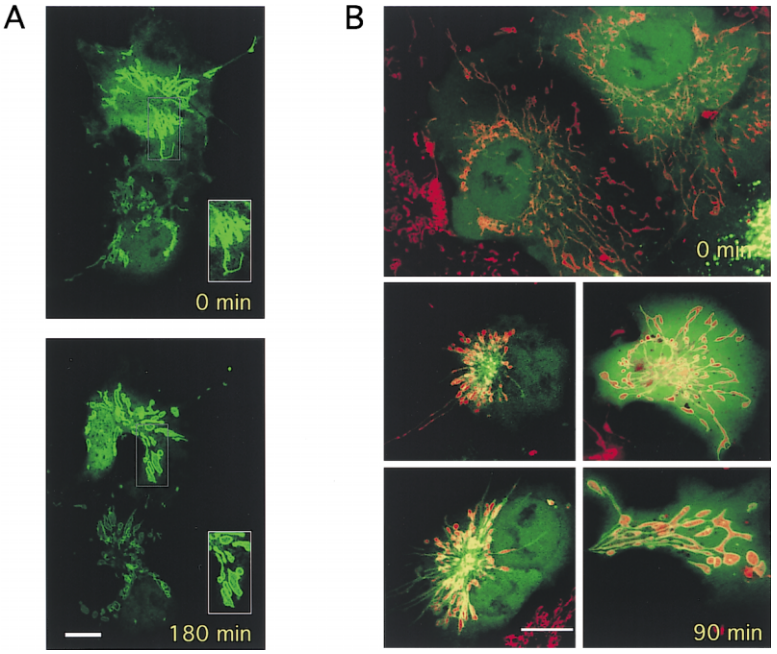

Figure 5. Drp_{K38A} Inhibits Mitochondrial Fragmentation Even When Full-Length Bax Is Overexpressed

(A) In COS-7 cells cotransfected with GFP-Bax and Drp_{K38A}, STS treatment leads to profound swelling of the mitochondria. Despite overexpression of proapoptotic Bax, which promotes the punctiform phenotype (see Figure 2), the disintegration of tubular mitochondria is negligible in cells concomitantly expressing the Drp_{K38A} mutant. Scale bar, 20 μm. (B) Staining of these cells with the membrane potential-sensitive dye MitoTracker red CMXRos reveals that swollen mitochondria (panels at bottom) retain their inner membrane potential. Scale bar, 20 μm.

The release of cytochrome c from the mitochondria into the cytosol (Liu et al., 1996) has been considered an important event for the activation of downstream caspases, and the recent report on the phenotype of cytochrome c knockout cell lines featuring reduced caspase 3 activation and resistance to various apoptotic stimuli including staurosporine (Li et al., 2000) is consistent with this paradigm. Drp1 mediates fission of the outer mitochondrial membrane that sequesters cytochrome c and other apoptogenic proteins from the cytosol in healthy cells. Therefore, we determined the effect of Drp_{K38A} expression on the release of endogenous cytochrome c. Immunohistochemical analyses of HeLa cervical carcinoma cells, performed after 3 hr of STS treatment, revealed that cells overexpressing Drp_{K38A} exhibit a punctate cytochrome c distribution, whereas in Drp_{wt}-overexpressing cells a diffuse cytosolic distribution, reflecting significant release of cytochrome c, was prevalent (Figure 6C). These observations were corroborated by subcellular fractionation experiments (Figure 6D). We therefore conclude that, by regulating loss of $\Delta\psi_m$ and mitochondrial cytochrome c release, Drp1 participates in cell death pathways acting at the level of or upstream of mitochondria.

Inhibition of Drp1 Function Blocks Apoptotic Cell Death

Having demonstrated that loss of $\Delta\psi_m$ as well as cytochrome c release require Drp1, we hypothesized that Drp1 may also participate in the mitochondrial control of apoptosis. To test this hypothesis, TUNEL was performed on STS-treated COS-7 cells transfected with either Drp_{wt} or Drp_{K38A}. We found that expression of Drp_{K38A} blocked apoptotic cell death: after 10 hr of STS treatment, 77% of Drp_{wt} transfected COS-7 cells were found to be TUNEL positive, as compared to 19% of Drp_{K38A} transfected cells (Figure 7A). To corroborate these data, we tested whether Drp_{K38A} expression was capable of inhibiting apoptosis triggered by various other inducers of mitochondria-dependent cell death. We found a marked attenuation of apoptosis in COS-7 cells transfected with Drp_{K38A} as compared to Drp_{wt} transfected cells 18 hr after γ irradiation (data not shown) as well as after 32 hr of treatment with the topoisomerase inhibitor etoposide (500 μM; Figure 7D). Inhibition of both γ irradiation- (200 Gy; Figure 7B) and STS-induced apoptosis by expression of Drp_{K38A} was also observed in SW480 human colon adenocarcinoma cells. After 18 hr of STS treatment, 64% of Drp_{wt} transfected SW480 cells were TUNEL positive, as compared to 24% of Drp_{K38A} transfected cells (data not shown). Finally, we show in Jurkat cells that anti-Fas-induced apoptosis and etoposide-induced apoptosis depend on Drp1 (Figure 7C). Interestingly, and in accordance with the current knowledge on Fas-mediated signaling, the apoptosis pathway induced by anti-Fas treatment that can partially bypass mitochondria (Scaffidi et al., 1998) is inhibited by Drp_{K38A} to a lesser degree (Drp_{wt}: 86% compared to Drp_{K38A}: 46%) than the etoposide-induced apoptosis pathway (Drp_{wt}: 96% compared to Drp_{K38A}: 5%).

Altogether, these results demonstrate that, by overexpression of a dominant-negative Drp1 mutant, various mitochondria-dependent cell death pathways can be inhibited. To corroborate this conclusion by independently testing the role of endogenous Drp1 in apoptosis, HeLa cells were microinjected with affinity-purified anti-Drp1 antibodies and subsequently treated with STS to induce cell death. Only 17% of the anti-Drp1 injected cells died by apoptosis at 20 hr of STS treatment as compared to 86% of cells injected with control antibody (Table 1). Moreover, the inhibition of apoptosis by microinjected anti-Drp1 was almost completely abolished by coinjection of excess peptide to which the anti-Drp1 antibody was raised. These results independently confirm the validity of conclusions drawn from Drp_{K38A} overexpression experiments. In summary, we conclude that

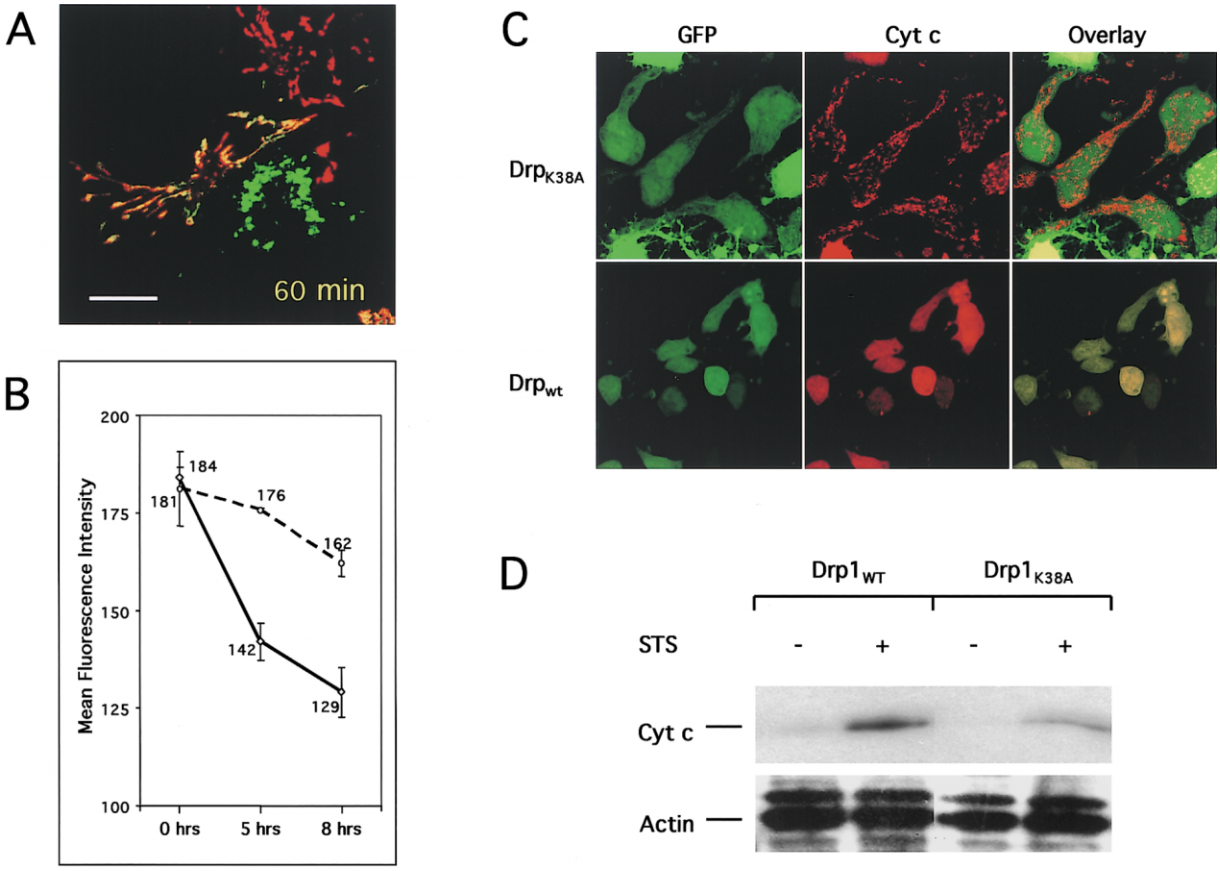

Figure 6. Loss of the Mitochondrial Membrane Potential $\Delta\psi_m$ Coincides with the Disintegration of the Mitochondrial Reticulum and Is, Together with the Release of Cytochrome C, Inhibited by Dominant-Negative Drp1

COS-7 cells cotransfected with mito-GFP and pcDNA3-Bax (to accelerate apoptosis) were stained with MitoTracker red CMXRos and visualized by confocal microscopy at 60 min after apoptosis induction (1.2 μM STS).

(A) The overlay image shows $\Delta\psi_m$-positive mitochondria of one cell in orange, whereas mitochondria of an adjacent cell have lost their membrane potential and appear green. Note that stretched mitochondria retain $\Delta\psi_m$ whereas most punctiform mitochondria do not. Scale bar, 20 μm.

(B) Loss of $\Delta\psi_m$ was quantified by flow cytometry analysis of Drp$_{wt}$ versus Drp$_{K38A}$ transfected COS-7 cells after STS treatment for indicated time periods (1.2 μM). Drp$_{wt}$ transfected cells (solid line) exhibit a significantly reduced $\Delta\psi_m$ at 5 hr, and loss of $\Delta\psi_m$ appears to be complete at about 8 hr of STS treatment. In contrast, Drp$_{K38A}$ transfected cells (hatched line) exhibit a much slower decline in membrane potential. The respective mean fluorescence intensity values in the graph (y dimension) represent the average values of triplicate samples.

(C) Apoptosis-associated cytochrome c release from mitochondria, induced by 3 hr of STS treatment, was comparatively analyzed by immunohistochemistry in HeLa cells cotransfected with pEGFP-C3 as transfection marker and either Drp$_{wt}$ or Drp$_{K38A}$. GFP/Drp$_{K38A}$ cotransfected cells (top panels) exhibit a mitochondrial cytochrome c (red) staining pattern, whereas in GFP/Drp$_{wt}$ cotransfected cells a diffuse cytosolic distribution is observed, consistent with the apoptosis-associated release of cytochrome c.

(D) The release of cytochrome c during apoptosis was analyzed by Western blotting in HeLa cells transfected with either Drp$_{wt}$ or Drp$_{K38A}$. Cells were treated with STS (1.2 μM) for 3 hr to induce apoptosis. Twenty-five micrograms of cytosolic protein was loaded per lane. Equal loading was confirmed with an anti-actin antibody.

Drp1 is an intrinsic component of multiple mitochondria-dependent apoptosis pathways.

Discussion

In this manuscript, we demonstrate that during apoptosis the mitochondrial reticulum of mammalian cells disintegrates into multiple punctiform organelles. We find that dynamin-related protein 1, a recently identified dynamin homolog, is causally involved in the profound switch of mitochondrial phenotypes. Furthermore, inhibition of Drp1 prevents the DNA fragmentation indicative of apoptotic cell death.

Based on reports that have implicated members of the dynamin family with membrane fission (recently reviewed by Hinshaw, 2000), we explored the role of the dynamin homolog Drp1 in mitochondrial fission during apoptosis. Under apoptotic conditions, Drp1 translocates to the mitochondria, and the typical reticular organization of worm-like mitochondria disintegrates into multiple small fragments. The apoptosis-associated translocation of Drp1 to potential mitochondrial constriction sites and mitochondrial tips resembles the pattern observed during mitochondrial division in *C. elegans* (Labrousse et al., 1999), consistent with the conclusion that Drp1 is involved in the transition from a tubular to a punctiform mitochondrial phenotype. This notion is corroborated by the fact that expression of a

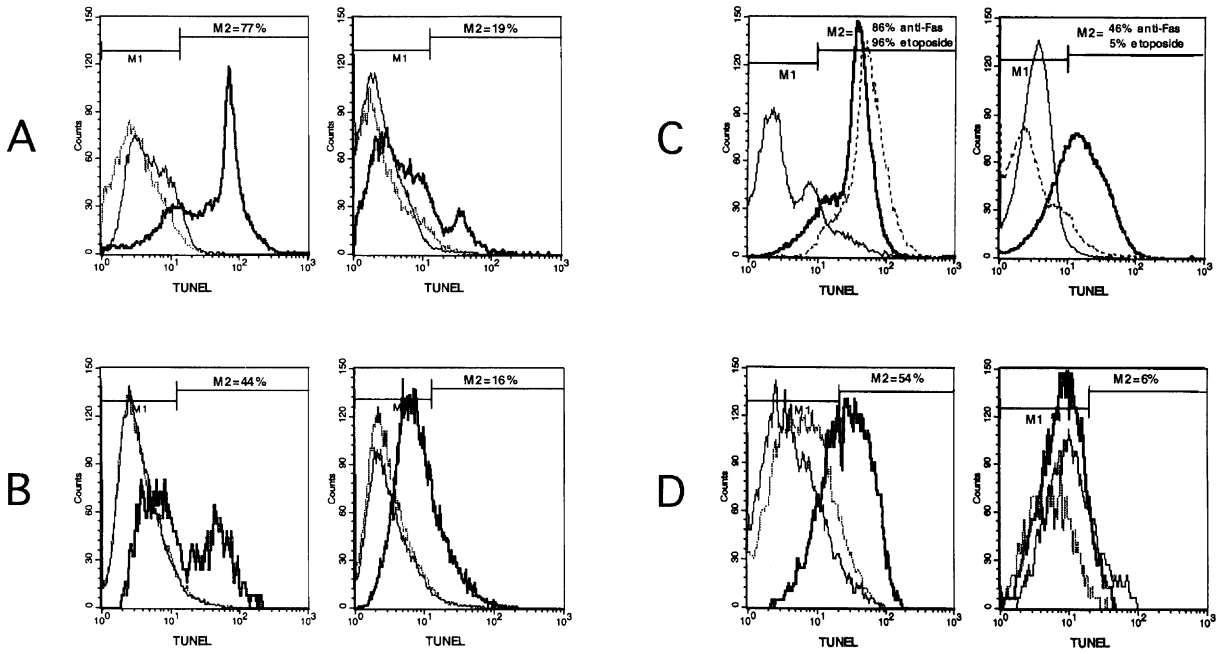

Figure 7. Expression of Dominant-Negative Drp1 Inhibits Apoptotic Cell Death

(A) Apoptosis as measured by TUNEL analysis was quantified in Drp_{wt} (left) versus Drp_{K38A} (right) transfected COS-7 cells after STS treatment (1.2 μM). Histogram overlays show TUNEL-positive cells at 0 (solid thin line) and 10 hr (solid thick line) after STS treatment. Seventy-seven percent of cells transfected with Drp_{wt} were found to be TUNEL positive, as compared to 19% of Drp_{K38A} transfected cells. In both panels, the dotted line denotes control staining (STS-treated Drp_{wt} [left] or Drp_{K38A} [right] transfected cells, incubated with reaction mix lacking terminal deoxynucleotidyl transferase).

(B) TUNEL analysis was performed in Drp_{wt} (left) versus Drp_{K38A} (right) transfected SW480 cells after γ irradiation (200 Gy). Histogram overlays show TUNEL-positive cells at 0 (solid thin line) and 18 hr (solid thick line) after irradiation. Forty-four percent of cells transfected with Drp_{wt} were found to be TUNEL positive as compared to 16% of Drp_{K38A} transfected cells. The dotted lines denote control staining.

(C) The effect of Drp_{K38A} overexpression on etoposide- and anti-Fas-induced apoptosis was analyzed in Jurkat cells. After 8 hr of anti-Fas treatment (solid thick line; 100 ng/ml), 86% of cells transfected with Drp_{wt} were found to be TUNEL positive as compared to 46% of Drp_{K38A} transfected cells. When etoposide was used to induce apoptosis (dotted line; 100 μM for 10 hr), cells transfected with Drp_{K38A} were even more protected (Drp_{wt}: 96% TUNEL-positive cells versus Drp_{K38A}: 5%). Solid thin line denotes TUNEL staining at 0 hr (control staining not shown).

(D) TUNEL analysis performed in COS-7 cells treated with 500 μM etoposide for 32 hr. Experimental conditions and graphical documentation otherwise identical to (A). Histograms (A)–(D) represent 10,000 gated cells and are representative of triplicate samples (y dimension = number of cells [counts]; x dimension [TUNEL] = relative fluorescence intensity measuring the extent of apoptotic DNA fragmentation).

dominant-negative mutant, Drp_{K38A}, blocks mitochondrial fission under apoptotic conditions. However, Drp_{K38A} transfected cells exhibit remarkable mitochondrial swelling, a component of various mechanistic apoptosis models (Kroemer and Reed, 2000). In light of conflicting data, it is still debatable whether swelling of the organelles is generally required for the mitochondrial release of certain proapoptotic proteins. Mitochondrial swelling has been described in several apoptosis pathways (Matsuyama et al., 2000; Petit et al., 1998; Scarlett et al., 2000), and Vander Heiden et al. (1997) reported that progressive mitochondrial swelling in response to a variety of apoptotic stimuli is regulated by the antiapoptotic Bcl-2 protein Bcl-x_L. On the other hand, absence of mitochondrial swelling during apoptosis has also been observed in several experimental systems (Jürgensmeier et al., 1998; Kluck et al., 1999; Martinou et al., 1999). We demonstrate here that, when mitochondrial fission is blocked by Drp_{K38A}, prominent swelling of the organelles can be readily visualized when augmented by Bax overexpression. It therefore appears that Drp1 controls the balance between mitochondrial swelling and fragmentation of the tubular organelles. This balance, that may vary in different cells and with different stimuli, may help explain some of the differences reported in the literature. During apoptosis, the initial swelling, either alone or in conjunction with stretching, may initiate mitochondrial accumulation of Drp1. Drp1 localized at the surface of mitochondria might then promote the fragmentation of the

Table 1. Inhibition of Apoptosis by Microinjection of Anti-Drp1 Antibody

Control antibody	86% ± 8%
Anti-Drp1 antibody	17% ± 3%
Anti-Drp1 antibody + excess competing peptide	72% ± 12%

HeLa cells were microinjected with either control FITC-labeled anti-rabbit antibody (0.4 mg/mL; top), affinity-purified anti-peptide antibody against Drp1 (amino acids 511–526; acetyl-NIEEQRRNRLAR ELPSC-amide; rabbit; 0.8 mg/mL; middle), or anti-peptide antibody against Drp1 (0.8 mg/mL) plus excess competing Drp1 peptide (1 mM; acetyl-NIEEQRRNRLARELPSC-amide; bottom). The specificity of the anti-Drp1 antibody was confirmed by Western blot and immunoprecipitation experiments performed on HeLa cell lysates (data not shown). Shown is the percentage of apoptotic cells at 20 hr after STS treatment (1.2 μM), as assessed by HOECHST staining.

organelles so that swelling (which would otherwise occur) cannot routinely be observed. However, by inhibiting Drp1 and simultaneously overexpressing Bax, a more pronounced swelling can be reproducibly visualized.

Despite the ability of dynamins to form multimeric spirals around the neck of nascent vesicles (Sever et al., 1999; Stowell et al., 1999; Sweitzer and Hinshaw, 1998; Takei et al., 1995), it is not entirely clear how certain dynamins exert their functions and how their activity is regulated. Functional analogies as well as sequence conservation would suggest that Drp1 and dynamins may employ similar mechanisms. Cytosolic Drp1 may cycle on and off mitochondria, analogous to dynamin cycling between the cytosol and the plasma membrane (Labrousse et al., 1999; Schmid et al., 1998). Regardless of the exact mechanism(s) of Drp1-dependent mitochondrial fragmentation, the fact that inhibition of Drp1 function (either by overexpressing a dominant-negative Drp1 mutant or by microinjecting anti-Drp1 antibodies) effectively blocks apoptotic cell death at the level of or upstream of mitochondria provides important insights as to how certain mitochondria-dependent apoptosis pathways might occur.

As suggested recently, various mechanisms for the apoptosis-induced release of proapoptotic proteins from the mitochondrial intermembrane space may exist (Green, 2000). A new hypothesis consistent with our data is that Drp1 may mediate vesicle formation at the outer mitochondrial membrane and that these vesicles may contain the mitochondrial intermembrane space proteins which translocate to the cytosol during cell death. However, it remains to be demonstrated that the mediation of apoptosis by Drp1 at least partly relies on the mechanochemical properties of certain dynamins.

Finally, it should also be taken into account that the list of proteins involved in the regulation of mitochondrial fusion and division is still growing at remarkable speed. The recent discovery of two new proteins that interact with Dnm1p, a yeast homolog of Drp1, to mediate mitochondrial fission (Cerveny et al., 2001; Fekkes et al., 2000; Mozdy et al., 2000; Tieu and Nunnari, 2000) not only underlines the complex nature of the apparatus required for mitochondrial division (reviewed by van der Bliek, 2000) but also indicates that Drp1 is unlikely to remain the only factor regulating mitochondrial fragmentation and associated events in mammalian cells undergoing apoptosis. Put into an even wider perspective, it is tempting to speculate that in addition to the known mechanisms for the degradation and disposal of various cellular constituents, one of Drp1's main functions may lie in the controlled disassembly of mitochondrial organelles during cell death.

Experimental Procedures

Cell Culture and Reagents

COS-7 green monkey renal epithelial cells, HeLa human cervical carcinoma cells, Jurkat T cell leukemia cells, and SW480 human colon adenocarcinoma cells (ATCC, Rockville, MD) were cultured at 37°C in 5% CO_2 in DMEM (COS-7, HeLa) and RPMI 1640 (Jurkat, SW480), respectively, supplemented with 10% fetal calf serum, 10 mM HEPES buffer (pH 7.0), 2 mM glutamine, nonessential amino acids, 2.5 μM sodium-pyruvate, 100 U/ml penicillin, and 100 μg/ml streptomycin. Media and antibiotics were obtained from Biofluid (Rockville, MD). HOECHST 33342 and mitochondria-specific dyes MitoTracker red CMXRos (MitoTracker) and 3,3-dihexyloxacarbocyanine iodide [$DiOC_6(3)$] were from Molecular Probes (Eugene, OR). The nonselective caspase inhibitor carbobenzoxy-valyl-alanyl-aspartyl(β-methyl ester)-fluoromethyl ketone (Z-VAD-fmk) was from Alexis Biochemicals (San Diego, CA), and the DNA Fragmentation Detection Kit from Oncogene Research Products (Cambridge, MA). Except where noted, all other reagents were obtained from Sigma Chemical (St. Louis, MO).

Expression Constructs

C3-EGFP-Bax and pcDNA3-Bax constructs have been described previously (Wolter et al., 1997). pcDNA3-BaxΔBH3 (BaxΔBH3, lacking amino acids 63–72 of human Bax) was generously provided by J.T. Ho (University of Washington, Seattle). Plasmids mito-GFP, C3-EYFP, and pDsRed1-N1 (DsRed) were from Clontech Laboratories (Palo Alto, CA). Human pcDNA3-Drp1 (Drp_{wt}) and dominant-negative mutant pcDNA3-Drp1K38A (Drp_{K38A}) were kindly provided by Drs. E. Smirnova and A.M. van der Bliek (University of California, Los Angeles) and have been described elsewhere (Smirnova et al., 1998). Drp_{wt} was recloned into C1-EGFP to yield GFP-Drp1. A C3-EYFP-Bax tail fusion construct that lacks Ser-184 within the C-terminal 21 amino acids of Bax was used as an outer mitochondrial membrane marker (YFP-$Baxtail_{\Delta 184}$). The C3-EGFP version of this nontoxic construct was previously described and identical restriction sites were used to reclone it into the C3-EYFP plasmid (Nechushtan et al., 1999).

Transfection Procedures

For confocal microscopy and immunohistochemistry, COS-7 and HeLa cells, respectively, were grown in 4.3 cm^2 chamber slides (2-well Lab-Tek chambered coverglass system; Nalge Nunc, Naperville, IL) and transfected using FuGENE6 transfection reagent (Roche Diagnostics GmbH, Mannheim, Germany) according to the manufacturer's instructions using 1.0 μg of total DNA per chamber. Cotransfections were performed in a 1:3 molar ratio of a combination of pEGFP-C3 and expression vectors. For flow cytometry analyses, COS-7 cells were grown in 6-well tissue culture plates; transfection procedures were identical, except that pDsRed1-N1 was used instead of pEGFP-C3 and 2.0 μg of total DNA were used per well.

Confocal Microscopy

Two-well chamber slides that allow the parallel and comparative imaging of two separately transfected cell populations under identical experimental conditions were used throughout the study. At 20 hr after transfection and at least 30 min prior to STS treatment, COS-7 cells were routinely exposed to the pan-caspase inhibitor Z-VAD-fmk at a concentration of 25 μM, and in indicated experiments 20 ng/ml of MitoTracker were added. Images prior to and at given time points after exposure to 1.2 μM STS were collected under thermostated conditions (37°C) using a LSM 510 model confocal microscope with a 63 × 1.4 NA apochromat objective (Carl Zeiss, Thornwood, NY). The 488 and 514 nm lines of an argon laser were used for fluorescence excitation of EGFP and EYFP, respectively. A helium/neon laser (543 nm) was used for excitation of MitoTracker. After acquisition, RGB images were processed using LSM 510 and Metamorph software.

All experiments aimed at the assessment and quantification of mitochondrial phenotypes were performed in a blinded manner (i.e., blinded transfections for unbiased image acquisition; encoded images assessed in random order by at least two independent investigators) and repeated at least twice independently. A punctiform mitochondrial phenotype after STS treatment was scored when at least 90% of the tubular mitochondria were disintegrated.

Electron Microscopy

Ultrastructural analyses were performed to quantify mitochondrial size in untreated versus STS-treated COS-7 cells. Cells were fixed with 2% paraformaldehyde and 2% glutaraldehyde in 0.1 M potassium cacodylate buffer for 30 min. After embedding in epoxy resin, cells were thin sectioned and visualized by electron microscopy.

Apoptosis Assays

Flow cytometry was used to comparatively quantify independent apoptosis-associated events in Drp_{wt} versus Drp_{K38A} transfected cells (COS-7, SW480, Jurkat cell lines). Two established cell death assays were performed: $DiOC_6(3)$ measurement reflecting alterations of the mitochondrial membrane potential $\Delta\psi_m$ (Kluck et al., 1997; Kroemer et al., 1998; Scaffidi et al., 1998; Susin et al., 1997; Zamzami et al., 1995), and terminal deoxynucleotidyl transferase-mediated dUTP-biotin nick-end labeling (TUNEL), quantifying apoptotic DNA fragmentation (Gorczyca et al., 1993) (Fluorescein-FragEL DNA Fragmentation Detection Kit, Oncogene Research Products, Cambridge, MA). In both assays, cotransfected cells (DsRed/Drp_{wt} and DsRed/Drp_{K38A}, respectively) were either incubated at 16 hr after transfection with various apoptotic stimuli (STS, etoposide, anti-Fas antibody [clone CH-11; from Immunotech, Marseille, France]) for indicated lengths of time or underwent γ irradiation (200 Gy). Cells assayed for loss of $\Delta\psi_m$ were then incubated with $DiOC_6(3)$ at 40 nM for 15 min. For the TUNEL assay, cells were washed in PBS, fixed in 2% paraformaldehyde (30 min at 4°C), and then resuspended and maintained in 70% ethanol overnight at −20°C. Cells were then washed in PBS, aliquoted, and incubated for 30 min at 37°C in 50 μl of a cacodylate reaction buffer/sample (consisting of 0.2 M potassium cacodylate, 25 mM Tris-HCl, pH 6.6, 2.5 mM cobalt chloride, 0.25 mg/ml BSA, and 0.5 nM biotin-16-dUTP) with or without 100 U/ml TdT (reagents from Boehringer Mannheim, Indianapolis, IN). Cells were then washed with PBS and resuspended in 100 μl of a saline sodium-citrate buffer/sample (supplemented with 5% nonfat dry milk and 0.1% Triton X-100) and streptavidin-FITC (2.5 μg/ml), followed by incubation for 30 min at RT in the dark. Cells were washed again in saline and analyzed immediately by flow cytometry for quantitation of TUNEL-positive cells. Data analysis was performed on 500–10,000 FL2-gated (i.e., transfected) cells using a Becton Dickinson FACScan. All analyses were done in triplicates and results confirmed by independent experiments.

In addition to $DiOC_6(3)$-staining and TUNEL, apoptosis-associated cytochrome c release from mitochondria was analyzed in HeLa cells by immunohistochemistry and conventional subcellular fractionation/Western blotting. The following antibodies were used: clone 6H2.B4 (PharMingen, San Diego, CA) and Texas red-labeled anti-mouse IgG (KPL Laboratories, Gaithersburg, MD) for immunohistochemical staining of cytochrome c, clone 7H8.2C12 (PharMingen) for cytochrome c detection by Western blotting, and an anti-actin antibody (Santa Cruz Biotechnology, Santa Cruz, CA) for demonstration of equal loading.

For subcellular fractionation, transfected cells (Drp_{wt} and Drp_{K38A}, respectively, each cotransfected with human HLA-A2 as a selection marker) were separated from untransfected cells by magnetic bead separation (LS-positive selection columns from Miltenyi Biotec, Bergisch Gladbach, Germany) using an anti-HLA-A2 monoclonal antibody (One Lambda, Canoga Park, CA) and goat anti-mouse IgG microBeads (Miltenyi Biotec). The technical procedures for immunohistochemistry and subcellular fractionation are described in detail elsewhere (Goldstein et al., 2000; Yang et al., 1997).

Microinjection experiments were performed on HeLa cells using a micromanipulator 5171 and a microinjector 5242 (Eppendorf, Hamburg, Germany) installed on an inverted microscope. Affinity-purified anti-Drp1 peptide antibody was kindly provided by C. Blackstone and M. Sheng (Harvard University Medical School, Boston, MA).

Cells were injected with either anti-Drp1 antibody (0.8 mg/mL), anti-Drp1 antibody plus excess competing peptide (1 mM), or with FITC-labeled anti-rabbit control antibody (0.4 mg/mL; Santa Cruz Biotechnology, Santa Cruz, CA). Texas red-labeled dextran of 70 kDa (Molecular Probes, Eugene, OR) at a concentration of 2 mg/mL was used as injection marker. In each experiment, at least 100 cells were injected per group. At 20 hr after STS treatment cells were assessed by HOECHST staining.

Acknowledgments

The authors thank E. Smirnova and A.M. van der Bliek for kindly providing the wild-type and dominant-negative Drp1 genes, C. Blackstone and M. Sheng for anti-Drp1 polyclonal antibodies, J.T. Ho for the BaxΔBH3 plasmid, and A. Nechushtan for the YFP-Bax-$tail_{\Delta 184}$ construct. We thank S. Cheng and V. Tanner-Crocker (NINDS EM Facility) for their excellent support with electron microscopy as well as Y. Lee and P. Johnson for valuable technical assistance. We are grateful to H. Arnheiter for critical reading and discussion of the manuscript. E.R. is an HHMI/NIH Research Scholar recipient. The generous gift from the Novartis foundation to S.F. is gratefully acknowledged.

Received November 27, 2000; revised August 31, 2001.

References

Adams, J.M., and Cory, S. (1998). The Bcl-2 protein family: arbiters of cell survival. Science *281*, 1322–1326.

Bleazard, W., McCaffery, J.M., King, E.J., Bale, S., Mozdy, A., Tieu, Q., Nunnari, J., and Shaw, J.M. (1999). The dynamin-related GTPase Dnm1 regulates mitochondrial fission in yeast. Nat. Cell Biol. *1*, 298–304.

Cerveny, K.L., McCaffery, J.M., and Jensen, R.E. (2001). Division of mitochondria requires a novel DNM1-interacting protein, Net2p. Mol. Biol. Cell *12*, 309–321.

Desagher, S., and Martinou, J.C. (2000). Mitochondria as the central control point of apoptosis. Trends Cell Biol. *10*, 369–377.

Fekkes, P., Shepard, K.A., and Yaffe, M.P. (2000). Gag3p, an outer membrane protein required for fission of mitochondrial tubules. J. Cell Biol. *151*, 333–340.

Goldstein, J.C., Waterhouse, N.J., Juin, P., Evan, G.I., and Green, D.R. (2000). The coordinate release of cytochrome c during apoptosis is rapid, complete and kinetically invariant. Nat. Cell Biol. *2*, 156–162.

Gorczyca, W., Gong, J., and Darzynkiewicz, Z. (1993). Detection of DNA strand breaks in individual apoptotic cells by the in situ terminal deoxynucleotidyl transferase and nick translation assays. Cancer Res. *53*, 1945–1951.

Green, D.R. (2000). Apoptotic pathways: paper wraps stone blunts scissors. Cell *102*, 1–4.

Green, D.R., and Reed, J.C. (1998). Mitochondria and apoptosis. Science *281*, 1309–1312.

Gross, A., Jockel, J., Wei, M.C., and Korsmeyer, S.J. (1998). Enforced dimerization of BAX results in its translocation, mitochondrial dysfunction and apoptosis. EMBO J. *17*, 3878–3885.

Gross, A., McDonnell, J.M., and Korsmeyer, S.J. (1999). BCL-2 family members and the mitochondria in apoptosis. Genes Dev. *13*, 1899–1911.

Hinshaw, J.E. (2000). Dynamin and its role in membrane fission. Annu. Rev. Cell Dev. Biol. *16*, 483–519.

Hsu, Y.T., Wolter, K.G., and Youle, R.J. (1997). Cytosol-to-membrane redistribution of Bax and Bcl-X(L) during apoptosis. Proc. Natl. Acad. Sci. USA *94*, 3668–3672.

Imoto, M., Tachibana, I., and Urrutia, R. (1998). Identification and functional characterization of a novel human protein highly related to the yeast dynamin-like GTPase Vps1p. J. Cell Sci. *111*, 1341–1349.

Jürgensmeier, J.M., Xie, Z., Deveraux, Q., Ellerby, L., Bredesen, D., and Reed, J.C. (1998). Bax directly induces release of cytochrome c from isolated mitochondria. Proc. Natl. Acad. Sci. USA *95*, 4997–5002.

Kamimoto, T., Nagai, Y., Onogi, H., Muro, Y., Wakabayashi, T., and Hagiwara, M. (1998). Dymple, a novel dynamin-like high molecular weight GTPase lacking a proline-rich carboxyl-terminal domain in mammalian cells. J. Biol. Chem. *273*, 1044–1051.

Kluck, R.M., Bossy-Wetzel, E., Green, D.R., and Newmeyer, D.D. (1997). The release of cytochrome c from mitochondria: a primary site for Bcl-2 regulation of apoptosis. Science *275*, 1132–1136.

Kluck, R.M., Esposti, M.D., Perkins, G., Renken, C., Kuwana, T., Bossy-Wetzel, E., Goldberg, M., Allen, T., Barber, M.J., Green, D.R., and Newmeyer, D.D. (1999). The pro-apoptotic proteins, Bid and Bax, cause a limited permeabilization of the mitochondrial outer membrane that is enhanced by cytosol. J. Cell Biol. *147*, 809–822.

Kroemer, G. (1997). The proto-oncogene Bcl-2 and its role in regulating apoptosis. Nat. Med. *3*, 614–620.

Kroemer, G., Dallaporta, B., and Resche-Rigon, M. (1998). The mitochondrial death/life regulator in apoptosis and necrosis. Annu. Rev. Physiol. *60*, 619–642.

Kroemer, G., and Reed, J.C. (2000). Mitochondrial control of cell death. Nat. Med. *6*, 513–519.

Labrousse, A.M., Zappaterra, M.D., Rube, D.A., and van der Bliek, A.M. (1999). C. elegans dynamin-related protein DRP-1 controls severing of the mitochondrial outer membrane. Mol. Cell *4*, 815–826.

Li, K., Li, Y., Shelton, J.M., Richardson, J.A., Spencer, E., Chen, Z.J., Wang, X., and Williams, R.S. (2000). Cytochrome c deficiency causes embryonic lethality and attenuates stress-induced apoptosis. Cell *101*, 389–399.

Liu, X., Kim, C.N., Yang, J., Jemmerson, R., and Wang, X. (1996). Induction of apoptotic program in cell-free extracts: requirement for dATP and cytochrome c. Cell *86*, 147–157.

Martinou, I., Desagher, S., Eskes, R., Antonsson, B., Andre, E., Fakan, S., and Martinou, J.C. (1999). The release of cytochrome c from mitochondria during apoptosis of NGF-deprived sympathetic neurons is a reversible event. J. Cell Biol. *144*, 883–889.

Matsuyama, S., Llopis, J., Deveraux, Q.L., Tsien, R.Y., and Reed, J.C. (2000). Changes in intramitochondrial and cytosolic pH: early events that modulate caspase activation during apoptosis. Nat. Cell Biol. *2*, 318–325.

McNiven, M.A., Cao, H., Pitts, K.R., and Yoon, Y. (2000). The dynamin family of mechanoenzymes: pinching in new places. Trends Biochem. Sci. *25*, 115–120.

Mozdy, A.D., McCaffery, J.M., and Shaw, J.M. (2000). Dnm1p GTPase-mediated Mitochondrial Fission Is a Multi-step Process Requiring the Novel Integral Membrane Component Fis1p. J. Cell Biol. *151*, 367–380.

Nechushtan, A., Smith, C.L., Hsu, Y.T., and Youle, R.J. (1999). Conformation of the Bax C-terminus regulates subcellular location and cell death. EMBO J. *18*, 2330–2341.

Nechushtan, A., Smith, C.L., Lamensdorf, I., Yoon, S.H., and Youle, R.J. (2001). Bax and Bak coalesce into novel mitochondria-associated clusters during apoptosis. J. Cell Biol. *153*, 1265–1276.

Otsuga, D., Keegan, B.R., Brisch, E., Thatcher, J.W., Hermann, G.J., Bleazard, W., and Shaw, J.M. (1998). The dynamin-related GTPase, Dnm1p, controls mitochondrial morphology in yeast. J. Cell Biol. *143*, 333–349.

Petit, P.X., Goubern, M., Diolez, P., Susin, S.A., Zamzami, N., and Kroemer, G. (1998). Disruption of the outer mitochondrial membrane as a result of large amplitude swelling: the impact of irreversible permeability transition. FEBS Lett. *426*, 111–116.

Pitts, K.R., Yoon, Y., Krueger, E.W., and McNiven, M.A. (1999). The dynamin-like protein DLP1 is essential for normal distribution and morphology of the endoplasmic reticulum and mitochondria in mammalian cells. Mol. Biol. Cell *10*, 4403–4417.

Rizzuto, R., Simpson, A.W., Brini, M., and Pozzan, T. (1992). Rapid changes of mitochondrial Ca2+ revealed by specifically targeted recombinant aequorin. Nature *358*, 325–327.

Scaffidi, C., Fulda, S., Srinivasan, A., Friesen, C., Li, F., Tomaselli, K.J., Debatin, K.M., Krammer, P.H., and Peter, M.E. (1998). Two CD95 (APO-1/Fas) signaling pathways. EMBO J. *17*, 1675–1687.

Scarlett, J.L., Sheard, P.W., Hughes, G., Ledgerwood, E.C., Ku, H.H., and Murphy, M.P. (2000). Changes in mitochondrial membrane potential during staurosporine-induced apoptosis in Jurkat cells. FEBS Lett. *475*, 267–272.

Schmid, S.L., McNiven, M.A., and De Camilli, P. (1998). Dynamin and its partners: a progress report. Curr. Opin. Cell Biol. *10*, 504–512.

Sesaki, H., and Jensen, R.E. (1999). Division versus fusion: Dnm1p and Fzo1p antagonistically regulate mitochondrial shape. J. Cell Biol. *147*, 699–706.

Sever, S., Muhlberg, A.B., and Schmid, S.L. (1999). Impairment of dynamin's GAP domain stimulates receptor-mediated endocytosis. Nature *398*, 481–486.

Shin, H.W., Shinotsuka, C., Torii, S., Murakami, K., and Nakayama, K. (1997). Identification and subcellular localization of a novel mammalian dynamin-related protein homologous to yeast Vps1p and Dnm1p. J. Biochem. *122*, 525–530.

Shpetner, H.S., and Vallee, R.B. (1989). Identification of dynamin, a novel mechanochemical enzyme that mediates interactions between microtubules. Cell *59*, 421–432.

Smirnova, E., Shurland, D.L., Ryazantsev, S.N., and van der Bliek, A.M. (1998). A human dynamin-related protein controls the distribution of mitochondria. J. Cell Biol. *143*, 351–358.

Smirnova, E., Griparic, L., Shurland, D.L., and van der Bliek, A.M. (2001). The dynamin-related protein Drp1 is required for mitochondrial division in mammalian cells. Mol. Biol. Cell, in press.

Stowell, M.H., Marks, B., Wigge, P., and McMahon, H.T. (1999). Nucleotide-dependent conformational changes in dynamin: evidence for a mechanochemical molecular spring. Nat. Cell Biol. *1*, 27–32.

Susin, S.A., Zamzami, N., Castedo, M., Daugas, E., Wang, H.G., Geley, S., Fassy, F., Reed, J.C., and Kroemer, G. (1997). The central executioner of apoptosis: multiple connections between protease activation and mitochondria in Fas/APO-1/CD95- and ceramide-induced apoptosis. J. Exp. Med. *186*, 25–37.

Susin, S.A., Zamzami, N., and Kroemer, G. (1998). Mitochondria as regulators of apoptosis: doubt no more. Biochim. Biophys. Acta *1366*, 151–165.

Sweitzer, S.M., and Hinshaw, J.E. (1998). Dynamin undergoes a GTP-dependent conformational change causing vesiculation. Cell *93*, 1021–1029.

Takei, K., McPherson, P.S., Schmid, S.L., and De Camilli, P. (1995). Tubular membrane invaginations coated by dynamin rings are induced by GTP-gamma S in nerve terminals. Nature *374*, 186–190.

Tieu, Q., and Nunnari, J. (2000). Mdv1p Is a WD Repeat Protein that Interacts with the Dynamin-related GTPase, Dnm1p, to Trigger Mitochondrial Division. J. Cell Biol. *151*, 353–366.

van der Bliek, A.M. (1999). Functional diversity in the dynamin family. Trends Cell Biol. *9*, 96–102.

van der Bliek, A.M. (2000). A mitochondrial division apparatus takes shape. J. Cell Biol. *151*, F1–F4.

Vander Heiden, M.G., Chandel, N.S., Williamson, E.K., Schumacker, P.T., and Thompson, C.B. (1997). Bcl-xL regulates the membrane potential and volume homeostasis of mitochondria. Cell *91*, 627–637.

Vander Heiden, M.G., and Thompson, C.B. (1999). Bcl-2 proteins: regulators of apoptosis or of mitochondrial homeostasis? Nat. Cell Biol. *1*, E209–E216.

Wang, K., Gross, A., Waksman, G., and Korsmeyer, S.J. (1998). Mutagenesis of the BH3 domain of BAX identifies residues critical for dimerization and killing. Mol. Cell. Biol. *18*, 6083–6089.

White, E. (1996). Life, death, and the pursuit of apoptosis. Genes Dev. *10*, 1–15.

Wolter, K.G., Hsu, Y.T., Smith, C.L., Nechushtan, A., Xi, X.G., and Youle, R.J. (1997). Movement of Bax from the cytosol to mitochondria during apoptosis. J. Cell Biol. *139*, 1281–1292.

Yang, J., Liu, X., Bhalla, K., Kim, C.N., Ibrado, A.M., Cai, J., Peng, T.I., Jones, D.P., and Wang, X. (1997). Prevention of apoptosis by Bcl-2: release of cytochrome c from mitochondria blocked. Science *275*, 1129–1132.

Yoon, Y., Pitts, K.R., Dahan, S., and McNiven, M.A. (1998). A novel dynamin-like protein associates with cytoplasmic vesicles and tubules of the endoplasmic reticulum in mammalian cells. J. Cell Biol. *140*, 779–793.

Zamzami, N., Marchetti, P., Castedo, M., Zanin, C., Vayssiere, J.L., Petit, P.X., and Kroemer, G. (1995). Reduction in mitochondrial potential constitutes an early irreversible step of programmed lymphocyte death in vivo. J. Exp. Med. *181*, 1661–1672.